ELSEVIER

Fusion Engineering and Design 41 (1998) 253–258

Fusion Engineering and Design

Design and construction of helical coils for LHD

S. Imagawa *, S. Masuzaki, N. Yanagi, S. Yamaguichi, T. Satow, J. Yamamoto, O. Motojima, LHD Group

National Institute for Fusion Science, Chikusa, Nagoya 464-01, Japan

Abstract

Helical coils for LHD are pool-cooled superconducting coils. In order to produce a fine magnetic surface, highly accurate manufacturing tolerances within ± 2 mm and high rigidity against large electro-magnetic forces are required. Additionally, high current densities of over 50 A mm^{-2} are necessary to keep enough distance between the helical coil and plasma. The helical coil is designed to enhance cryogenic stability by optimizing the wetted surface fraction of each conductor in considering both the magnetic field and stress in the insulator between conductors. For attaining highly accurate helical winding and cryogenic stability, composite conductors with pure aluminum stabilizers were developed and directly wound on highly accurate thick cases. The actual winding was carried out on-site from January 1995 to May 1996. After that, the top covers of the case were set on the coils and welded very carefully. The entire assembly was installed into an outer supporting shell. © 1998 Elsevier Science S.A. All rights reserved.

1. Introduction

The large helical device (LHD) is a fusion experimental apparatus with a pair of helical coils and three pairs of vertical field coils (poloidal coils), which will demonstrate a high-performance plasma usable to a fusion reactor design [1]. Accuracy of the position of coils is very important for magnetic fusion devices to produce a fine magnetic surface. In the LHD, the accuracy of the position for each coil is required to be within ± 2 mm, that is, corresponding to 5×10^{-4} of the major radius of 3.9 m. This value is derived to reduce the width of undesirable magnetic islands to one-tenth of the plasma minor radius for the most severe mode of deformations [2]. Additionally, the deformation of the current-center of each coil caused by electromagnetic force is required to be less than 1.9 mm at the central toroidal magnetic field $B_0 = 3$ T, that is, 3.4 mm at $B_0 = 4$ T. Furthermore, high current density is required for the helical coils to keep enough distance between the coil and the plasma. The average current density was required to be higher than 50 A mm^{-2} at $B_0 = 4$ T.

Since the amplitude of the varying magnetic field is small in the helical coils except during shut-off of the coil current, the restriction for coupling losses was not severe. To attain highly accurate helical shaping and winding, we selected pool-cooled medium-size conductors, which are directly wound on highly accurate cases (HC cans). A pure aluminum stabilizer was adopted to perform high recovery current. Since it is impossi-

* Corresponding author.

PII S0920-3796(97)00178-6

ble to withstand large electromagnetic force by the conductors themselves, they are packed into the HC cans which are finally supported by an outer shell structure 100 mm thick. The can is used as a bath for liquid helium. The major parameters and cross-sectional view of the helical coil are shown in Table 1 and Fig. 1, respectively. This paper is intended to summarize the design and the results of the construction of the helical coils.

2. Mechanical design of the supporting structure and helical coils

The mechanical design criteria and design conditions of LHD are shown in Table 2. The evaluation of stress was based on ASME section III, and crack growth and stress intensity factor were also evaluated. The largest amplitude of electromagnetic forces occurs by coil charge and discharge. Since the helical coil current will be ramped up in the morning and kept constant during day time, the number of cycles will be less than 2100, which allows partial welding for highly accurate assembling.

Table 1
Major parameters of the helical coil

Item	Phase I	Phase II
Bath temperature (K)	~4.4	~1.8
Central toroidal field (T)	3	4
Maximum field in coil (T)	6.9	9.2
Nominal current (kA)	13.0	17.3
Critical current (kA)	>22	>32
Current density of coil (A mm^{-2})	40	53
Magnetic stored energy (GJ)	0.92	1.64
Voltage to earth (V)	±1181	±1574
Major/minor radius (m)	3.9/0.975	3.9/0.975
Superconductor	Al-stabilized NbTi/Cu	Al-stabilized NbTi/Cu
Surface treatment	Oxidized	Oxidized
Number of turns	450	450
Size of conductor (mm)	12.5 × 18.0	12.5 × 18.0

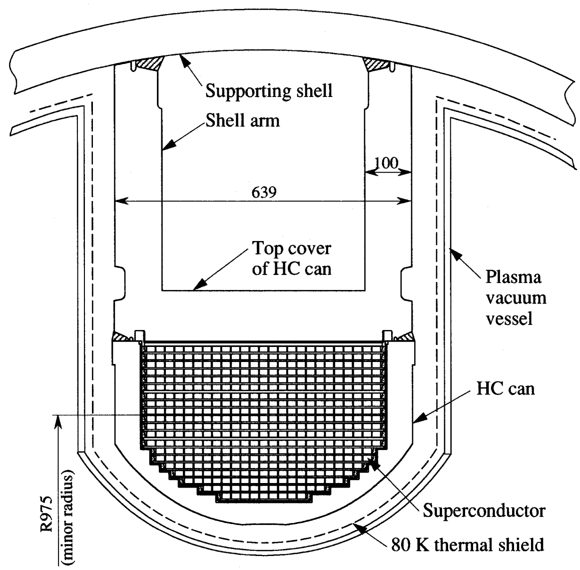

Fig. 1. Cross-section of the helical coil.

The electromagnetic force on the helical coil is divided into a minor-radius-hoop component and an overturning component. Since the poloidal coils cancel the vertical field caused by the helical coils themselves, the minor-radius-hoop force is dominant and uniform at standard operation modes. To estimate the loads acting on the supporting shell, the forces of the helical coils can be separated into a major-radius-hoop force and an

Table 2
Mechanical design criteria and condition

Design criteria	
Accuracy of coil position (mm)	<2
Deformation of coil by force (mm)	<1.9 (at $B_0 = 3$ T)
Stress in structures	Based on ASME section III
Crack growth (mm)	<1
Representative design conditions	
Cooling down (cycles)	32
Coil excitation (cycles)	2100
Operation mode transition (cycles)	310 000
Coil excitation time (h)	24 000
Plasma disruption: 150 kA, 1 ms (no. of times)	1000
Current shut-off (no. of times)	100
Earthquake: 0.3 G (no. of times)	10

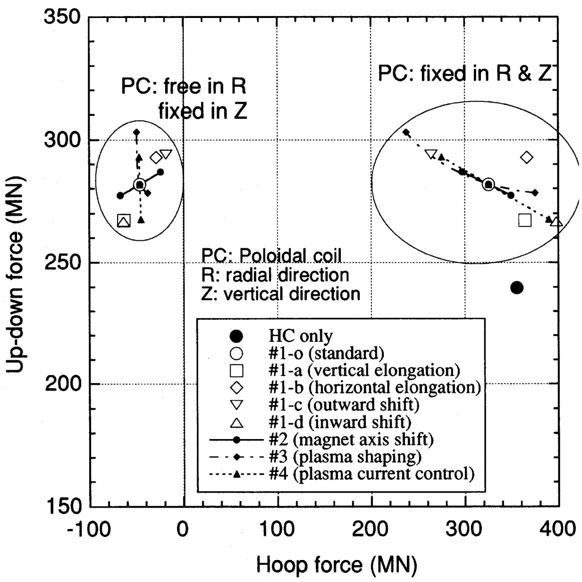

Fig. 2. Electromagnetic hoop and up–down forces on the supporting shell of helical coils at 4 T operations.

up–down force like poloidal coils by dividing them into upper and lower halves. Fig. 2 shows the forces acting on the supporting shell at the representative 4 T operations in two cases in which the poloidal coils are fixed and free to the shell in the radial direction. In the latter case, the poloidal coil must withstand the hoop force by itself. The largest total hoop force is only 10% larger than the hoop force of the helical coils in 'HC only' mode. Accordingly, the total weight of the supporting structures for all coils should be the least in the former case. Structural analyses were carried out of the supporting structures [3]. By considering rigidity of the poloidal coils, the maximum displacement and stress in the supporting structure are calculated to be 2.62 mm and 290 MPa at 4 T operation, respectively. The displacement of the current-center of each coil is estimated to be within 3.4 mm, including its own shrinkage. The maximum stress intensity appears at the corner of the aperture for the outer horizontal port of the plasma vacuum vessel. The value is within the allowable limit of SUS316 which is employed as the structural material of the supporting structures.

From the aspects of stability and reliability as a superconducting coil, the motion of the conductors due to electromagnetic forces must be small, that is, the rigidity of the coil must be high. The helical coil will be shrunk and shifted outwards by the electromagnetic force. By approximating it to a circular coil with average curvature, the movement and stress in each conductor was calculated by using a finite element method [4]. The electromagnetic force was applied on the center node of each conductor. Inner materials of the composite conductor, which were super-conducting strands, CuNi-clad pure aluminum and solder, were represented by a homogeneous element. Since the yield strength of pure aluminum is around 20 MPa, Young's modulus of the inner region of the conductor mainly depends on the rigidity of the insulator between conductors. We have developed an insulator with high rigidity and small thermal contraction. Young's modulus is larger than 22 GPa, and the compressive strength is over 1000 MPa. In the case of the rigidity of 22 GPa and the constant spacer factor of 0.5, the movement of the lowest layer and the maximum stress in the conductor were calculated to be 1.1 mm and 173 MPa, respectively. Since the fabrication gaps between the conductor and the insulator will be collapsed by the large electromagnetic forces, the gaps decrease the equivalent rigidity of the coil. The effect was evaluated by assuming that the total gaps are equal to the increase of the displacement of the lowest layer. The larger the gaps are, the higher is the stress in the conductor. The average fabrication gap was specified to be within 65 μm per layer to keep the stress in the copper sheath of conductors under the yield strength of 290 MPa. By attaining this condition, we will be able to avoid the coil quench caused by plastic deformation of the conductors.

3. Cryogenic stability of helical coils

Cryogenic stability is most important for large-scale superconducting coils. First of all, we developed composite conductors with high stability [5]. The critical current and recovery current of all actual conductors were measured by straight short samples. Next, we designed the cooling channels in the coil and optimized the wetted surface fraction of each conductor. The HC can is used as a bath for liquid helium, which is supplied from five inlets at the bottom of the coil. Gas helium is taken out from five outlets at the top connected to a header tank, liquid level inside which will be controlled. Longitudinal cooling channels inside the coils are arranged at the higher ends of each layer and both top corners, the areas of which are 30 and 300 mm^2, respectively. Electrical insulators between conductors are settled at intervals to create transverse cooling channels. The thicknesses of the insulator between turns and between layers are 2.0 and 3.5 mm, respectively.

The transverse component of the magnetic field is highest at the edge of the helical coil and becomes gradually lower toward the core. On the contrary, the load per unit length on each insulator between the conductors is the largest in the core and becomes smaller towards the edge. The wetted surface fraction of conductors, therefore, can be enlarged at the edge region in order to enhance the recovery current without enlarging stress in the insulators [6]. In actual winding, the width of each insulator was changed. In considering productivity, the number of steps of width of each layer to layer insulator was limited to within three. The wetted surface fraction of each conductor varies from 0.417 to 0.692 as shown in Fig. 3,

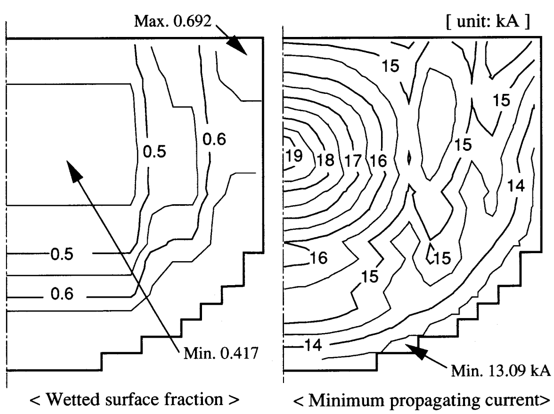

Fig. 3. Wetted surface fraction of each conductor and minimum propagating current calculated by Maddock's equal area theorem.

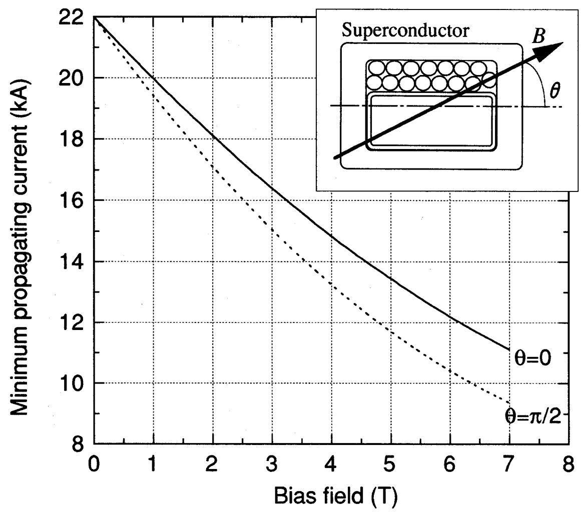

Fig. 4. Calculated minimum propagating current of the helical coil conductor at wetted surface fraction of 0.5.

and the smallest recovery current will be 15% higher than that in the case of a constant fraction of 0.5, assuming the heat transfer coefficient to be independent of the size of the wetted surface. By using the minimum propagating current, shown in Fig. 4, calculated from the measured heat transfer and best-fitted magneto-resistance, the recovery current at 3 T operation of each conductor was calculated as shown in Fig. 3 [7]. The minimum value was 13.09 kA, which was almost equal to the nominal current. In this evaluation, the heat transfer and magneto-resistance were assumed to be typical values, but both will be varied in actuality, and some region may exist where the minimum propagating current is less than the nominal current. Still, the helical coil will be operated stably, because almost all the conductors satisfy the cryostable condition.

4. Manufacturing helical coils

Because of the regulation for transportation on the road, the helical coils were wound on-site. In order to maintain accuracy while winding, we adopted the method to wind the conductors directly on the HC cans which were manufactured with a high precision of 0.50 mm as standard deviation. Besides, we developed the winding machine with 13 numerically controlled driving axes. We have also developed a method to apply the winding tension up to 50 MPa to the conductor by lateral shifting, and the conductor was prevented from floating from the lower insulator. Furthermore, we filled the room-temperature-cured resin under the layer to layer insulator as shown in Fig. 5, and the effective residual gap becomes half of the relief by slant.

On-site winding was carried out continuously from January 1995 to May 1996. It took 16 months to wind up the whole conductors of 36 km length. The maximum relief by slant of each conductor was controlled to under 0.30 mm by the reshaping process, and the average relief of each layer was successfully kept within 0.13 mm. The average gaps between layers were then attained within 65 μm. At the 19th layer, we measured the elastic modulus of the coil and confirmed that the required values were obtained. The position of the conductor in the overturning direction was controlled by the thickness of cotters at both sides, and the errors were suppressed to within ± 0.5 mm. The increase of the minor radius has an apparent tendency that it is large on the inside. The reasons are the geometrical increase and decline of shaping accuracy caused by the larger torsion angle. This component corresponds to a decrease of the major radius, which was only 0.25 mm among the 20 layers. The standard deviation of the differences of minor radii in each layer was kept to within 0.35 mm. Still, the difference between the average minor radii of each layer of two helical coils was kept to within 0.2 mm. We have attained the required winding accuracy. After winding, the top covers of the HC cans with arms have been set on the coils and welded very carefully. After that, the outer parts of the plasma vacuum vessel were fixed tentatively on the winding core. The entire assembly was set into the supporting shell, and the arms were welded to the shell. We came up with new ideas for each welding to protect the coil and to suppress deformation. According to the law of propagation of errors, the standard deviation (σ) of errors for position of all conductors is estimated to be 0.60 mm after finishing winding. The deformation of the HC cans caused by each welding should be kept under 1 mm to keep 3σ within 2 mm finally.

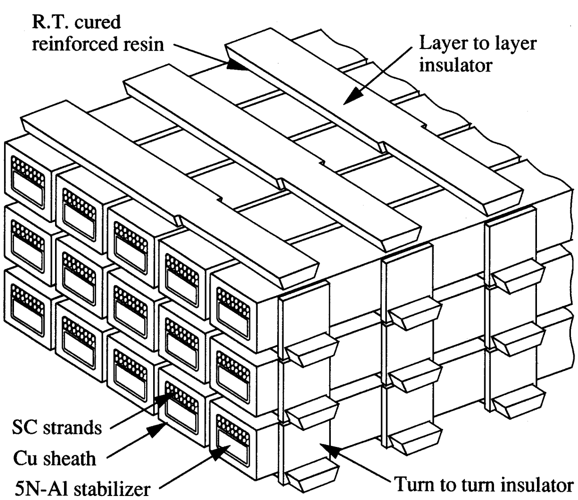

Fig. 5. Schematic drawing of a part of the helical coil.

5. Conclusion

The major requirements for the helical coils of the LHD are: (1) highly accurate manufacturing to within ± 2 mm, (2) high current density of over 50 A mm^{-2}, and (3) small deformation against electromagnetic force. By developing composite conductors with a pure aluminum stabilizer and by optimizing the wetted surface fraction of each conductor, the helical coils will be cryostable at 4.4 K for 3 T operation. From structural analyses, the deformation of the current-center of the coil was confirmed to satisfy the allowable value of 3.4 mm at 4 T operation. By developing a special winding machine and new methods to machine the layer to layer insulator by measured profile and to apply tension to the conductors, we completed on-site winding successfully. Furthermore, we have the confidence to be able to attain the accuracy of the coil position to within ± 2 mm by applying new ideas for each welding.

References

[1] O. Motojima, N. Yanagi, S. Imagawa, et al., Superconducting magnet design and construction of LHD, Plasma Phys. Controlled Nucl. Fusion Res. (1996) F1-Cn-64/G2-4.

[2] K. Yamazaki, N. Yanagi, H. Ji, H. Kaneko, N. Ohyabu, T. Satow, S. Morimoto, J. Yamamoto, O. Motojima, The LHD Design Group, Requirements for accuracy of superconducting coils in the large helical device, Fusion Eng. Des. 20 (1993) 79–86.

[3] S. Imagawa, H. Hayashi, H. Tamura, A. Nishimura, T. Satow, J. Yamamoto, O. Motojima, The LHD Group, Structural analysis of the large helical device, Adv. Cryogenic Eng. A 39 (1994) 309–316.

[4] S. Imagawa, N. Yanagi, S. Yamaguchi, T. Satow, J. Yamamoto, O. Motojima, T. Senba, S. Suzuki, K. Nakanishi, K. Asano, T. Yamagiwa, The LHD Group, Construction of helical coil winding machine for LHD and on-site winding, IEEE Trans. Magn. 32 (4) (1996) 2248–2251.

[5] N. Yanagi, T. Mito, K. Takahata, M. Sakamoto, A. Nishimura, S. Yamada, S. Imagawa, H. Kaneko, J. Yamamoto, O. Motojima, Experimental observation of anomalous magnetoresistivity in 10–20 kA class aluminum stabilized superconductors, Adv. Cryogenic Eng. 40 (1994) 459–468.

[6] S. Imagawa, N. Yanagi, T. Satow, J. Yamamoto, O. Motojima, The LHD Group, Optimization of wetted surface fraction of helical coils for LHD, Cryogenics 34 (ICEC Suppl.) (1994) 701–704.

[7] S. Imagawa, N. Yanagi, T. Mito, T. Satow, J. Yamamoto, O. Motojima, The LHD group, Evaluation of recovery current of the helical coil for LHD, ICEC16/ICMC, Kitakyushu, Japan, May 20–24, 1996, OC7-5.